Design of Non-redundant Sparse Planar Arrays with Reduced Mutual Coupling

Hangqi Yan, *Student Member, IEEE*, Yuexian Wang, *Member, IEEE*, Ling Wang, *Member, IEEE*, Rongfeng Li, and Wei Liu, *Senior Member, IEEE*

***Abstract*—Most existing sparse planar arrays cannot fully realize their potential in terms of the degrees-of-freedom (DOFs) due to redundancies in their co-array generation. Meanwhile, the small inter-element spacing in conventional planar arrays may cause serious mutual coupling effects. In this paper, a series of designs for non-redundant sparse planar arrays in different application scenarios are proposed. They can obtain the maximum possible DOFs under the constraints of area and the number of array elements. We first present the rule for non-redundancy design for planar arrays, which is the basic criterion for the following optimization problems. According to generalized disjunctive programming (GDP), we establish systematic solutions for array designs by two mixed-integer linear programming (MILP) optimization approaches. Then, three classes of non-redundant planar arrays are designed to achieve minimum area, pre-determined area, and reduced mutual coupling, respectively. In particular, the non-redundant planar arrays with reduced mutual coupling can be designed to both avoid small inter-element spacing and obtain the minimum area, which makes them more robust to mutual coupling conditions. Simulation results are provided to demonstrate the superiority of the proposed planar array configurations for direction-of-arrival (DOA) estimation.**

***Index Terms*—Non-redundant array, planar array, virtual array, mixed-integer linear programming, direction-of-arrival estimation.**

I. Introduction

Planar arrays, also known as two-dimensional (2D) arrays, are widely used for 2D direction-of-arrival (DOA) estimation in wireless communications, underwater acoustic localization, radar, emitters tracking, etc [1]-[9]. Over the past few years, the vast majority of research has focused on uniform planar arrays, including uniform rectangular arrays (URAs), uniform circular arrays (UCAs), hexagonal arrays, and parallel-shaped arrays [2]. However, these array structures have small inter-element spacing between adjacent elements, which may cause severe mutual coupling effects [10]; they also have a smaller number of degrees-of-freedom (DOFs) due to the uniform nature of their geometry configurations.

Recently, many studies have focused on nonuniform arrays to extend the inter-element spacing and reduce mutual coupling effectively. Among them, one-dimensional (1D) sparse arrays have received wide attentions [11]-[16], and several typical nonuniform linear arrays (NLAs) have been designed, such as coprime arrays (CA) [17] and nested arrays (NA) [18]. The CA is composed of two sub-arrays with their number of sensors being a coprime pair. It provides a large number of unique virtual lags with reduced mutual coupling, while the NA can provide more continuous virtual arrays with denser array elements. Based on them, several other NLAs have been developed for different purposes, including increasing the number of consecutive or unique lags, reducing mutual coupling effects, limiting array aperture, etc [19]-[22].

Inspired by these typical NLAs, several nonuniform planar arrays (NPAs) have been proposed for 2D DOA estimation. Parallel linear arrays are one of the classical categories, including parallel coprime array (PCA) [23], parallel nested array (PNA) [24], and others [25], [26]. Based on parallel linear arrays, many 2D DOA estimation algorithms have been designed for improving estimation accuracy, reducing variables and computational complexity [26], [27]-[29]. Non-parallel linear arrays are another type of array configurations. For instance, the conventional cross array is composed of two uniform linear arrays which are connected at the middle point of each array orthogonally. The improved cross-shaped array is considered for mixed source localization [30]. In [31], the L-shaped array is discussed, which has higher accuracy than the conventional cross array. Then, the NLAs are applied to sub-arrays of the L-shaped array [32], [33]. In [34], the V-shaped coprime (VCA) and the V-shaped nested array (VNA) configurations are developed, which are able to use fewer array elements to estimate the same number of sources. Another typical 2D array with hole-free virtual array was proposed in [35], [36]. However, these aforementioned NPAs cannot achieve the highest DOFs due to redundancy in their unique lags.

To obtain more unique virtual lags, there have been a lot of interests in studying and designing non-redundant sparse arrays [37], [38]-[40]. Arsac *et al*. considered the minimum-redundancy array (MRA), and they design array configurations that constructed the largest possible linear virtual array with zero redundancy [41]. The sensors are placed sparsely and each inter-element spacing only appears once except for position zero. Moreover, Vertatschitsch *et al*. employed

This work is supported by National Natural Science Foundation of China under Grant No. 61971357 and No. 62271412. (*Corresponding author: Yuexian Wang; Ling Wang*.)

H. Yan, Y. Wang, and L. Wang are with the School of Electronics and Information, Northwestern Polytechnical University, Xi'an, 710072, China. (e-mail: crookes@mail.nwpu.edu.cn; yuexian.wang@nwpu.edu.cn; lingwang@nwpu.edu.cn).

R. Li is with the Research on Applied Acoustics in Hangzhou. (email: gothicer@yeah.net).

W. Liu is with the School of Electronic Engineering and Computer Science, Queen Mary University of London, E1 4NS London, U.K. (e-mail: wliu.eee@gmail.com).

the exhaustive search method to provide non-redundant 1D arrays with minimum missing lags [39]. For sensors more than four, the lags are unavoidable and the inter-element spacing is discontiguous. Linebarger *et al*. introduced several relationships about the bounds on the number of redundancies in arrays [40]. As a result, the exhaustive search operation can be simplified by using such prior information. However, if the number of sensors becomes large, the exhaustive search method is still time-consuming and impractical.

The non-redundant array designs mentioned above mainly aim at linear arrays and has achieved some results. In this paper, our work focuses on the design of non-redundant planar arrays, i.e., generalizing the 1D case to 2D. To simplify the discussion, we first convert the 2D coordinates of the array elements to 1D unique data sets and develop the design rule for non-redundant planar arrays. Based on practical requirements, especially the array area and mutual coupling effects, different formulations are considered for non-redundant planar arrays.

To modify search methods and reduce computation time, generalized disjunctive programming (GDP) can provide a solution for optimization problems involving both discrete and continuous variables [42], [43]. The GDP can be relaxed by Boolean and continuous variables, which is an alternative expression to the conventional algebraic mixed-integer programming formulation [42]. Mixed-integer linear programming (MILP) can convert GDP to corresponding integer counterparts, and it is able to handle the problem that some variables are continuous while others are integers. The development of these optimization methods has been growing fast over the past years [44], [45]. We consider using GDP and MILP formulations to solve the design problem in our work.

The main contributions of this paper are summarized as follows:

1) A design rule for non-redundant sparse planar arrays is provided to ensure maximum possible DOFs of $N^2-(N-1)$ DOFs for N array elements.

2) Based on the above rule, a disjunctive programming framework is developed. Two MILP methods, the convex hull and the big M-representation, are considered to solve the disjunctive programming problems for generalized 2D array designs. The proposed optimization methods can speed up the search by adding more restrictive constraints.

3) Three classes of novel non-redundant planar arrays are designed. The first non-redundant planar array can obtain the minimum array area with a fixed size of one edge of a rectangular region. The second array can adapt to any determined $P \times Q$ rectangular region, where P and Q are positive integers. The third one is designed to reduce mutual coupling effects which provides larger array element spacing than other classical 2D arrays.

The remaining part of this paper is organized into five sections. Section II provides some preliminaries about signal model, virtual array, mutual coupling, and DOA estimation. We introduce the rule for non-redundant sparse planar array design and two MILP methods for enhanced non-redundant planar array designs in Section III. In Section IV, the design of the proposed sparse planar arrays under specific conditions is presented. In Section V, simulation results are provided. Eventually, conclusions are drawn in Section VI.

Notations: $(\cdot)^*, (\cdot)^T$, and $(\cdot)^H$ represent conjugate, transpose, and conjugate-transpose, respectively. $\|\cdot\|_k, k = 1, 2$ stands for ℓ_k-norm. $\otimes$ and $\odot$ denote the Kronecker product and Khatri-Rao product, respectively. The vectorization operator is represented by $\mathrm{vec}(\cdot)$. Moreover, $\mathbf{I}_N$ represents the $N \times N$ identity matrix and $\mathbf{1}_N$ represents the $N \times 1$ column vectors of all ones. For matrix $\mathbf{Y}$, $\mathbf{y}^{(h)}$ is its hth row and $\mathbf{Y}^{[h]}$ is the matrix formed by removing the hth row from $\mathbf{Y}$. The inequality $\mathbf{Y} \overset{e}{\neq} \mathbf{Z}$ indicates that the elements of the corresponding rows of $\mathbf{Y}$ and $\mathbf{Z}$ are not equal. $\Omega(\cdot)$ is a logical operator that returns $True$ when the condition is met.

II. Preliminaries

A. Signal Model

A planar array with N antennas is considered, with coordinates of antennas as $\mathbf{L}d = \left[\mathbf{L}_1^T, \mathbf{L}_2^T, ..., \mathbf{L}_N^T\right]^T d$, in which $\mathbf{L}_i = [x_i, y_i]^T \in \mathbb{Z}^2$ is an integer-valued vector and $d = \lambda/2$ is the unit inter-element spacing with λ being the signal wavelength. K far field, narrowband, and uncorrelated sources impinge on the planar array from azimuth angles $\theta_i \in [0, 2\pi]$ and elevation angles $\varphi_i \in [0, \pi/2], i = 1, 2, ..., K$. Consequently, the received signal vector can be written as

$$\mathbf{x}(t) = \mathbf{A}(\theta, \varphi)\mathbf{s}(t) + \mathbf{n}(t) \tag{1}$$

where $\mathbf{s}(t) = [s_1(t), ..., s_K(t)]$ is the source vector and $\mathbf{n}(t)$ represents the noise vector following an additive white Gaussian process. The matrix $\mathbf{A}(\theta, \varphi) = [\mathbf{a}(\theta_1, \varphi_1), ..., \mathbf{a}(\theta_K, \varphi_K)]$ denotes the array mainfold, where the steering vector $\mathbf{a}(\theta_i, \varphi_i)$ is expressed as

$$\begin{array}{c}\mathbf{a}(\theta_i, \varphi_i) = [1, e^{-j(x_1 \cos\theta_i \sin\varphi_i + y_1 \sin\theta_i \sin\varphi_i)\frac{2\pi}{\lambda}}, \\ ..., e^{-j(x_N \cos\theta_i \sin\varphi_i + y_N \sin\theta_i \sin\varphi_i)\frac{2\pi}{\lambda}}]^T\end{array} \tag{2}$$

where $j = \sqrt{-1}$.

From (1), the covariance matrix is given by

$$\begin{aligned}\mathbf{R}_{\mathbf{x}} &= \mathrm{E}\left[\mathbf{x}(t)\mathbf{x}^H(t)\right] \\ &= \textstyle\sum_{i=1}^{K} \sigma_i^2 \mathbf{a}(\theta_i, \varphi_i)\mathbf{a}^H(\theta_i, \varphi_i) + \sigma_n^2 \mathbf{I}_N \\ &= \mathbf{A}(\theta, \varphi)\mathbf{R}_{\mathbf{s}}\mathbf{A}^H(\theta, \varphi) + \sigma_n^2 \mathbf{I}_N\end{aligned} \tag{3}$$

where $\mathbf{R}_{\mathbf{s}} = \mathrm{E}\left[\mathbf{s}(t)\mathbf{s}^H(t)\right] = \mathrm{diag}\left(\left[\sigma_1^2, \sigma_2^2, ..., \sigma_K^2\right]\right)$ is the source covariance matrix, and σ_i^2 denotes the power of the ith source. In practice, $\mathbf{R}_{\mathbf{x}}$ can only be estimated by a limited number of snapshots as

$$\widetilde{\mathbf{R}}_{\mathbf{x}} = \frac{1}{T}\sum_{t=1}^{T} \mathbf{x}(t)\mathbf{x}^H(t) \tag{4}$$

B. Virtual Array

To take full advantage of the covariance matrix $\widetilde{\mathbf{R}}_{\mathbf{x}}$, we consider to vectorize it into an $N^2 \times 1$ column vector $\mathbf{r}$, which is written as

$$\mathbf{r} = \mathrm{vec}\left(\widetilde{\mathbf{R}}_{\mathbf{x}}\right) = \bar{\mathbf{A}}(\theta, \varphi)\mathbf{g} + \bar{\sigma}_n^2 \mathrm{vec}(\mathbf{I}_N) \tag{5}$$

where $\bar{\mathbf{A}}(\theta,\varphi)=[\bar{\mathbf{a}}(\theta_1,\varphi_1),....,\bar{\mathbf{a}}(\theta_K,\varphi_K)]$ with $\bar{\mathbf{a}}(\theta_i,\varphi_i)=\mathbf{a}^*(\theta_i,\varphi_i)\otimes\mathbf{a}(\theta_i,\varphi_i)$, and $\mathbf{g}=\left[\sigma_1^2,\sigma_2^2,...,\sigma_K^2\right]^T$. Therefore, the mth element in $\bar{\mathbf{a}}(\theta_i,\varphi_i)$ can be simplified as

$$\mathbf{V}(m)=e^{-j[(x_q-x_p)\cos\theta_i\sin\varphi_i+(y_q-y_p)\sin\theta_i\sin\varphi_i]\frac{2\pi}{\lambda}} \tag{6}$$

where $x_p, x_q, y_p,$ and y_q are the coordinates of physical antennas. Eq. (6) gives an example of a virtual array element located at position $[x_q-x_p, y_q-y_p]^T$.

Hence, the set of generated virtual array can be defined by

$$\mathbb{V}=\{\mathbf{L}_p-\mathbf{L}_q \mid \mathbf{L}_p,\mathbf{L}_q\in\mathbf{L}\} \tag{7}$$

C. Mutual Coupling

The mutual coupling effect is not considered in previous signal model (1). With mutual coupling, (1) can be modified to

$$\mathbf{x}(t)=\mathbf{C}\mathbf{A}(\theta,\varphi)\mathbf{s}(t)+\mathbf{n}(t) \tag{8}$$

where $\mathbf{C}\in\mathbb{C}^{N\times N}$ stands for the mutual coupling matrix, which is co-defined by many factors. In the 2D model, the elements in $\mathbf{C}$ can be expressed as [36]

$$\langle\mathbf{C}\rangle_{\mathbf{L}_i,\mathbf{L}_j}=\begin{cases}c\left(\|\mathbf{L}_i-\mathbf{L}_j\|_2\right) & \|\mathbf{L}_i-\mathbf{L}_j\|_2\le B\\ 0 & \|\mathbf{L}_i-\mathbf{L}_j\|_2>B\end{cases} \tag{9}$$

where $c(\cdot)$ denotes the mutual coupling coefficient and B is the maximum separation between antenna pairs assuming the presence of mutual coupling effects. $c(0)=1$ and $|c(k)/c(\ell)|=\ell/k$ are defined as in [10]. If the array element spacing increases, the mutual coupling effect will decrease. Therefore, the following weight function can be used to measure the influence of mutual coupling [46].

Definition 1. (Weight function): The weight function $w(\mathbf{m})$ for 2D arrays is defined as the number of sensor pairs with spacing $\mathbf{m}\in\mathbb{V}$.

$$w(\mathbf{m})=w(m_x,m_y)=\left|\left\{(\mathbf{L}_1,\mathbf{L}_2)\in\mathbb{Z}^2 \mid \mathbf{L}_1-\mathbf{L}_2=\mathbf{m}\right\}\right| \tag{10}$$

The magnitude of the weight function indicates the level of mutual coupling. If the mutual coupling effect is low, the value of weight function is small. Obviously, $\sqrt{m_x^2+m_y^2}$ is equal to the spacing between sensor pairs. In planar array, we mainly consider the value of $\mathbf{W}=(w(0,1),w(1,0),w(1,1),w(1,-1))$, where $\mathbf{W}$ is defined to simplify the representation.

D. DOA Estimation Method

We briefly review the sparse reconstruction method for DOA estimation in this part, which can use all the virtual array elements. From (5), each row in $\mathbf{r}$ can be regarded as a virtual array element located at set $\mathbb{V}$, and we can construct a virtual steering vector, corresponding to the difference co-array $\mathbb{V}$. According to [47], [48], the 2D DOA can be estimated by

$$\min\|\mathbf{g}\|_1 \qquad \text{s.t.}\left\|\mathbf{r}-\bar{\mathbf{A}}\mathbf{g}\right\|_2\le\kappa \tag{11}$$

where $\bar{\mathbf{A}}$ is the $N^2\times G$ over-complete dictionary with $G\gg K$, G is the size of search grid, and κ is a small error term. Therefore, the objective function with a regularized expression is given by

$$\hat{\mathbf{g}}=\underset{\mathbf{r}}{\operatorname{argmin}}\left\|\mathbf{r}-\bar{\mathbf{A}}\mathbf{g}\right\|_2+\mu\|\mathbf{g}\|_1 \tag{12}$$

where μ is a regularization parameter that balances the ℓ_1-norm and ℓ_2-norm terms.

III. Non-redundant Sparse Planar Arrays

The non-redundant planar array can obtain the maximum possible DOFs with a fixed number of antennas. The number of DOFs of a sparse array is the cardinality of its difference co-array in this paper. All the virtual array elements in $\mathbb{V}$ are unique except for the position at $(0,0)$. Considering a sparse planar array with N elements, a total number of N^2 virtual elements can be generated through the principle of difference co-array. Since the self-difference co-arrays by the physical antennas are all located at $(0,0)$, there exist $N-1$ redundant zero lags. Hence, an N-element non-redundant planar array can provide N^2-N+1 achievable DOFs (unique virtual array elements) in theory.

A. Design Rule for Non-redundant Sparse Planar Arrays

According to (7), if different pairs of sparse planar array elements generate the same difference co-array in the same position, it will lead to redundancy. However, redundancy at position $(0,0)$ is inevitable, so this part is ignored in the discussion. Assume that the difference co-array formed by a pair of array elements is unequal to that of another pair of array elements, and we then have

$$\mathbf{L}_i-\mathbf{L}_j\neq\mathbf{L}_m-\mathbf{L}_n,\quad i\neq m, i\neq j, m\neq n \tag{13}$$

where $i,j,m,n\in[1,N]$. The inequality is to make sure that the positions of difference co-array are nonzero. However, compared to the linear array case, the positions of planar array elements are 2D variables, which are more difficult to be analyzed. To simplify the discussion, assume that all array elements are distributed in a $P\times Q$ rectangular region, where P and Q are positive integers. The first array element is placed at the origin $(0,0)$. In Fig. 1, we can convert the 2D coordinates of the array element to a 1D unique ordinal number. Therefore, the design rule for non-redundant sparse planar arrays can be expressed as

$$\begin{cases}\eta_i+1\le\eta_{i+1} & i=1,2,...,N-1\\ \eta_j-\eta_k\neq\eta_m-\eta_n & j\neq m, j\neq k, m\neq n\end{cases} \tag{14}$$

where $\eta_i=Qx_i+y_i$, and x_i and y_i are the horizontal and vertical coordinates, respectively. According to (14), we can generate sparse planar arrays without redundancy.

B. Design of Enhanced Non-redundant Sparse Planar Arrays

In this subsection, we consider to improve the optimization problem on the design of non-redundant sparse planar arrays. According to [38], this work can also be formulated as an MILP problem. It is necessary to construct appropriate constraints for specific scenarios to obtain optimal planar arrays.

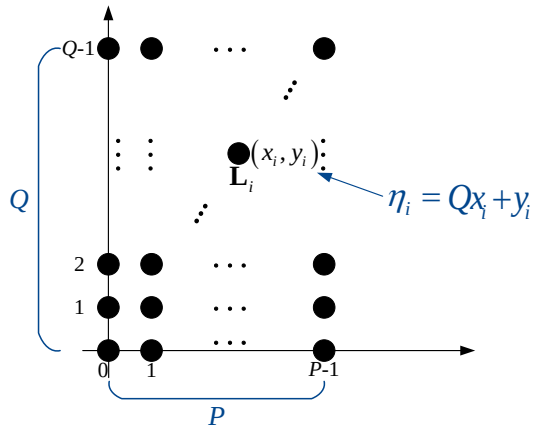

Fig. 1. The structure of a planar array.

In practice, if the array area is too large, it will increase the cost and the size of the carrying platform. Therefore, it is necessary to restrict the array area. The array elements are considered to be placed in the region of $P \times Q$. Moreover, since the rectangular boundaries P and Q are equivalent, only the case of $P \geq Q$ needs to be discussed. Therefore, we can simplify the rule in (14) as follows,

$$\begin{array}{lll} \min & x_N & \\ \text{s.t.} & \eta_i + 1 \leq \eta_{i+1} & i = 1, 2, ..., N-1 \\ & \eta_i - \eta_j \neq \eta_m - \eta_n & i \neq j, m \neq n, i \neq m \end{array} \tag{15}$$

where x_N is the horizontal coordinate of the Nth element. Obviously, we have $\max(x_i) = x_N, i \in [1, N]$. Therefore, we can achieve the minimum array area under a fixed Q.

We only need to focus on half of the virtual array elements, because the difference co-array is symmetric about the origin. In this way, the search size is reduced while the same difference co-array can still be obtained. Here, assume $i > j$ and $m > n$ to make sure that we do not need to search the symmetric part of the array elements. Hence, (15) can be rewritten as

$$\begin{array}{lll} \min & x_N & \\ \text{s.t.} & \eta_i + 1 \leq \eta_{i+1} & i = 1, 2, ..., N-1 \\ & \eta_i - \eta_j \neq \eta_m - \eta_n & i > j, m > n, i \neq m \end{array} \tag{16}$$

Next, define an $(N-1) \times 2N$ selection matrix $\mathbf{B}$, where $\mathbf{B}_{(k,k)} = -\mathbf{B}_{(k,k+3)} = -Q$ and $\mathbf{B}_{(k,k+1)} = -\mathbf{B}_{(k,k+2)} = -1$ for $k \in [1, N-1]$. To ensure that the array elements are unique and arranged in ascending order, we introduce the following inequality constraint

$$\mathbf{BL} \geq \mathbf{1}_{N-1} \tag{17}$$

where $\mathbf{L}$ is a $2N \times 1$ column vector. (17) satisfies the condition $\eta_i + 1 \leq \eta_{i+1}$ in (16) as a disjunction. In order to satisfy the uniqueness condition of virtual array elements, we need to define another $N(N-1)/2 \times 2N$ matrix $\mathbf{U}$, given by

$$\mathbf{U} = \left[\mathbf{U}_1^T, \mathbf{U}_2^T, ..., \mathbf{U}_N^T\right]^T \tag{18}$$

where

$$\mathbf{U}_n = \left[\mathbf{O}_{N-n,2(n-1)}, -\mathbf{v} \odot \mathbf{1}_{N-n}, \mathbf{I}_{N-n} \otimes \mathbf{v}\right], n \in [1, N-1] \tag{19}$$

with $\mathbf{v} = [2Q-1, 1]$.

For better understanding, we give an example to explain the structures of $\mathbf{B}$ and $\mathbf{U}$. With $N = 4$ and $Q = 2$, they are expressed as

$$\mathbf{B} = \begin{bmatrix} -2 & -1 & 2 & 1 & 0 & 0 & 0 & 0 \\ 0 & 0 & -2 & -1 & 2 & 1 & 0 & 0 \\ 0 & 0 & 0 & 0 & -2 & -1 & 2 & 1 \end{bmatrix} \tag{20}$$

$$\mathbf{U} = \begin{bmatrix} -3 & -1 & 3 & 1 & 0 & 0 & 0 & 0 \\ -3 & -1 & 0 & 0 & 3 & 1 & 0 & 0 \\ -3 & -1 & 0 & 0 & 0 & 0 & 3 & 1 \\ 0 & 0 & -3 & -1 & 3 & 1 & 0 & 0 \\ 0 & 0 & -3 & -1 & 0 & 0 & 3 & 1 \\ 0 & 0 & 0 & 0 & -3 & -1 & 3 & 1 \end{bmatrix} \tag{21}$$

The column vector $\mathbf{UL}$ gives all possible combinations of the difference co-array. However, the arrangement of elements in vector $\mathbf{UL}$ is irregular, and there may be redundancies. To avoid redundancy in difference co-array except for element zero, we compare all the generated difference co-array elements to each other. Then, the following inequality condition is set

$$\mathbf{1}_{H-1}\mathbf{u}^{(h)}\mathbf{L} \overset{e}{\neq} \mathbf{U}^{[h]}\mathbf{L}, \quad h \in [1, H] \tag{22}$$

where $H = N(N-1)/2$. After traversing the values of h, we can construct the extended matrix, which is given by

$$\hat{\mathbf{U}} = \begin{bmatrix} \mathbf{1}_{H-1}\mathbf{u}^{(1)} \\ \mathbf{1}_{H-1}\mathbf{u}^{(2)} \\ \vdots \\ \mathbf{1}_{H-1}\mathbf{u}^{(H)} \end{bmatrix} \text{ and } \check{\mathbf{U}} = \begin{bmatrix} \mathbf{U}^{[1]} \\ \mathbf{U}^{[2]} \\ \vdots \\ \mathbf{U}^{[H]} \end{bmatrix} \tag{23}$$

The dimension of both matrices $\hat{\mathbf{U}}$ and $\check{\mathbf{U}}$ is $D \times 2N$ with $D = H(H-1)$. Therefore, (22) can be further written as

$$\hat{\mathbf{U}}\mathbf{L} \overset{e}{\neq} \check{\mathbf{U}}\mathbf{L} \tag{24}$$

Moreover, we can obtain $\hat{\mathbf{u}}^{(d)}\mathbf{L} \neq \check{\mathbf{u}}^{(d)}\mathbf{L}, d \in [1, D]$ as another representation of (24). With (17) and (24), we can represent (16) as a generalized disjunctive programming problem [42], and it can be expressed as

$$\begin{array}{ll} \min & x_N \\ \text{s.t.} & \mathbf{BL} \geq \mathbf{1}_{N-1} \\ & \Omega\left(\hat{\mathbf{u}}^{(d)}\mathbf{L} \neq \check{\mathbf{u}}^{(d)}\mathbf{L}\right) = True \quad d = 1, ..., D \end{array} \tag{25}$$

According to (14) and (16), the above disjunctive programming problem (25) can guarantee a non-redundant difference co-array. Considering that both sides of the condition of logical operator are calculated as integers, it can rewritten as

$$\left[-1 \geq \hat{\mathbf{u}}^{(d)}\mathbf{L} - \check{\mathbf{u}}^{(d)}\mathbf{L}\right] \quad \vee \quad \left[\hat{\mathbf{u}}^{(d)}\mathbf{L} - \check{\mathbf{u}}^{(d)}\mathbf{L} \geq 1\right] \tag{26}$$

where $\vee$ indicates a logical OR operator.

We can then reformulate (25) as

$$\begin{array}{lll} \min\limits_{\forall \delta_d \in \{0,1\}, d \in [1,D]} & x_N & \\ \text{s.t.} & \mathbf{BL} \geq \mathbf{1}_{N-1} & \\ & \begin{bmatrix} \delta_d \\ \mathbf{f}^{(d)}\mathbf{L} \leq -1 \end{bmatrix} \quad \vee & \begin{bmatrix} 1-\delta_d \\ \mathbf{f}^{(d)}\mathbf{L} \geq 1 \end{bmatrix} \end{array} \tag{27}$$

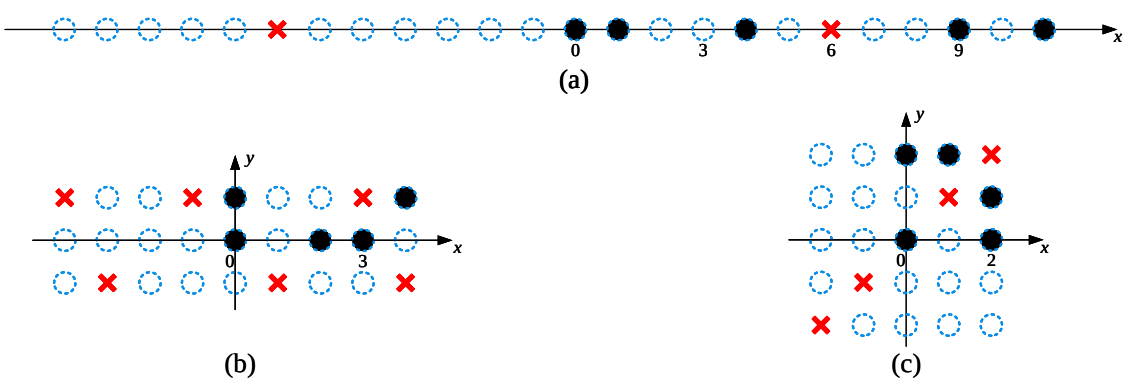

Fig. 2. The non-redundant array geometries with $N = 5$ elements: (a) $Q = 1$, (b) $Q = 2$, and (c) $Q = 3$.

where δ_d is an integer, 0 or 1. Define $\mathbf{F} = \hat{\mathbf{U}} - \check{\mathbf{U}}$ with $\mathbf{f}^{(d)} = \hat{\mathbf{u}}^{(d)} - \check{\mathbf{u}}^{(d)}$. If $\delta_d = 1$, the left-hand inequality is true. While $\delta_d = 0$, the right-hand inequality is satisfied. Then, we can form a column vector $\boldsymbol{\delta} = [\delta_1, ..., \delta_D]^T$.

It can be seen that (27) is a GDP problem and contains integer variables $\mathbf{L}$. However, most existing GDP solvers are only applicable to continuous variables and do not work with (27). To solve such problems efficiently, MILP is employed, which can handle mixed integer variables, as a substitution to GDP. Inevitably, due to the addition of integer variables, the computational complexity increases, and we need to relax the optimization problems by using partial prior conditions. We consider two approaches to transform (27) into MILP, named the convex hull and the big M-representation [43]. Although the solution is the same for both approaches, the difference between the two approaches is that the solution space of the convex hull is smaller, so the number of iterations is less. Nonetheless, it has more variables compared with the big M-representation, and a slower convergence rate. Both can be solved using existing MILP solvers [49], [50].

1) The convex hull: To achieve non-redundant sparse planar array design, the convex hull formulation is written as

$$\begin{aligned} \min_{\forall \delta_d \in \{0,1\}, d \in [1,D]} \quad & x_N \\ \text{s.t.} \quad & \mathbf{BL} \geq \mathbf{1}_{N-1} \\ & -\delta_d \geq \mathbf{f}^{(d)} \mathbf{L}_a \geq -M\delta_d \\ & M(1-\delta_d) \geq \mathbf{f}^{(d)} \mathbf{L}_b \geq 1 - \delta_d \\ & \mathbf{L}_a + \mathbf{L}_b = \mathbf{L} \end{aligned} \tag{28}$$

where $\mathbf{L}_a$ and $\mathbf{L}_b$ are intermediate variables and their sum is equal to $\mathbf{L}$. M is a sufficiently large positive number defined by users. When $\delta_d = 0$, $0 \geq \mathbf{f}^{(d)} \mathbf{L}_a \geq 0$ represents that $\mathbf{L}_a$ is zero. Similarly, the elements in $\mathbf{L}_b$ are zero when $\delta_d = 1$. Hence, this method increases the number of variables by adding intermediate variables.

2) The big M-representation: The big M-representation is given by

$$\begin{aligned} \min_{\forall \delta_d \in \{0,1\}, d \in [1,D]} \quad & x_N \\ \text{s.t.} \quad & \mathbf{BL} \geq \mathbf{1}_{N-1} \\ & \mathbf{f}^{(d)} \mathbf{L} \geq 1 - M\delta_d \\ & -1 + M(1-\delta_d) \geq \mathbf{f}^{(d)} \mathbf{L} \end{aligned} \tag{29}$$

When $\delta_d = 0$, we have $\mathbf{f}^{(d)} \mathbf{L} \geq 1$, and $-1 \geq \mathbf{f}^{(d)} \mathbf{L}$ is satisfied with $\delta_d = 1$. Furthermore, the inequalities are clearly valid and redundant when $\mathbf{f}^{(d)} \mathbf{L} \geq 1 - M, \delta_d = 1$ and $-1 + M \geq \mathbf{f}^{(d)} \mathbf{L}, \delta_d = 0$. If the value of M in (28) and (29) is too large, it will lead to an increase in computations. On the other hand, a small M can cause the optimization problem unsolvable. As suggested by [38] and [40], $M = N^2$ is a reasonable choice.

IV. Proposed Planar Array Designs

We design enhanced non-redundant planar arrays in this section subject to the size of array area, mutual coupling effect, etc. The first non-redundant planar array is designed to obtain the minimum array area with a fixed size for one side of the planar array. The second array can achieve the design for a pre-determined array area. The last one is for reducing mutual coupling effects.

A. Non-redundant Planar Arrays with Minimum Area

In this subsection, under the condition that $Q = \bar{Q}$, we design sparse planar arrays satisfying the minimum array area without redundancy. (16) can be rewritten as

$$\begin{aligned} \min \quad & x_N \\ \text{s.t.} \quad & Q = \bar{Q} && \bar{Q} \in \mathbb{Z}^+ \\ & \eta_i + 1 \leq \eta_{i+1} && i = 1, 2, ..., N-1 \\ & \eta_i - \eta_j \neq \eta_m - \eta_n && i > j, m > n, i \neq m \end{aligned} \tag{30}$$

Clearly the array becomes a 1D linear array when $Q = 1$. Therefore, non-redundant linear array is a special case of optimization problem (30). More generally, we can obtain the non-redundant planar array with the minimum area under different number of array elements N and different values of Q.

The formulation of the convex hull with a certain $\bar{Q}$ can be expressed as

$$\begin{aligned} \min_{\forall \delta_d \in \{0,1\}, d \in [1,D]} \quad & x_N \\ \text{s.t.} \quad & Q = \bar{Q} \\ & \mathbf{BL} \geq \mathbf{1}_{N-1} \\ & -\delta_d \geq \mathbf{f}^{(d)} \mathbf{L}_a \geq -M\delta_d \\ & M(1-\delta_d) \geq \mathbf{f}^{(d)} \mathbf{L}_b \geq 1 - \delta_d \\ & \mathbf{L}_a + \mathbf{L}_b = \mathbf{L} \end{aligned} \tag{31}$$

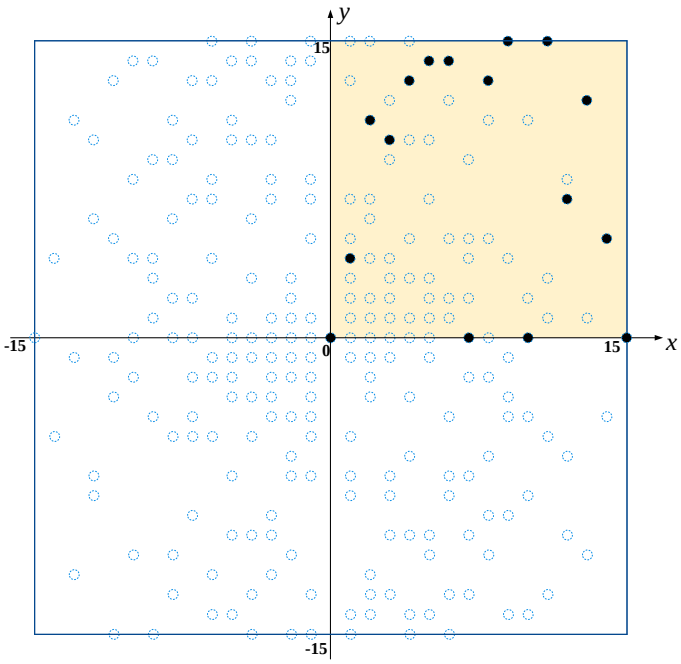

Fig. 3. The non-redundant planar array with fixed array area ($N = 16$, $Q = 16$, and $\bar{P} = 16$).

Similarly, we can express the big M-representation formulation as follows

$$\begin{aligned} \min_{\forall \delta_d \in \{0,1\}, d \in [1,D]} \quad & x_N \\ \text{s.t.} \quad & Q = \bar{Q} \\ & \mathbf{BL} \geq \mathbf{1}_{N-1} \\ & \mathbf{f}^{(d)}\mathbf{L} \geq 1 - M\delta_d \\ & -1 + M(1-\delta_d) \geq \mathbf{f}^{(d)}\mathbf{L} \end{aligned} \tag{32}$$

The above inequalities meet the requirement of designing minimum-area non-redundant sparse planar arrays with a fixed $\bar{Q}$, and it is worth noting that the solutions satisfying the condition of minimum area are usually not unique.

An example is given in Fig. 2. The solid black circles denote the physical array antenna positions, the dashed blue circles denote the positions of virtual array elements, and the red crosses stand for holes. The number of array elements is $N = 5$. It can be observed that when $Q = 1$ in (a) , we can obtain the optimization problem for 1D arrays, which is specifically analyzed in [38]. The minimum array aperture is equal to 11. Similarly, in Fig. 2 (b) and (c), the non-redundant sparse planar arrays with minimum area can be obtained under the fixed $Q = 2$ and $Q = 3$, respectively. The array area is 10 for $Q = 2$ and 9 for $Q = 3$.

B. Non-redundant Planar Arrays with Fixed Array Area

In the previous section, we discussed array configurations with minimum area that can be achieved, and obtained the corresponding minimum value of $P = P_{\min}$. Considering practical requirements, define $\bar{P}$ as the size for proposed array such that $\bar{P} \geq P_{\min}$, and two MILP optimization problems can be established. The convex hull formulation is given by

$$\begin{aligned} \max_{\forall \delta_d \in \{0,1\}, d \in [1,D]} \quad & x_N \\ \text{s.t.} \quad & Q = \bar{Q} \\ & x_N \leq \bar{P} \\ & \mathbf{BL} \geq \mathbf{1}_{N-1} \\ & -\delta_d \geq \mathbf{f}^{(d)}\mathbf{L}_a \geq -M\delta_d \\ & M(1-\delta_d) \geq \mathbf{f}^{(d)}\mathbf{L}_b \geq 1 - \delta_d \\ & \mathbf{L}_a + \mathbf{L}_b = \mathbf{L} \end{aligned} \tag{33}$$

Similarly, the formulation of the big M-representation can be expressed as

$$\begin{aligned} \max_{\forall \delta_d \in \{0,1\}, d \in [1,D]} \quad & x_N \\ \text{s.t.} \quad & Q = \bar{Q} \\ & x_N \leq \bar{P} \\ & \mathbf{BL} \geq \mathbf{1}_{N-1} \\ & \mathbf{f}^{(d)}\mathbf{L} \geq 1 - M\delta_d \\ & -1 + M(1-\delta_d) \geq \mathbf{f}^{(d)}\mathbf{L} \end{aligned} \tag{34}$$

Fig. 3 shows design examples with 16 elements, where $Q = 16$ and $\bar{P} = 16$. The solid black circles denote the physical array antenna positions and the dashed blue circles denote the positions of virtual array elements.

C. Non-redundant Planar Arrays with Reduced Mutual Coupling

When the inter-element spacing is small, mutual coupling cannot be ignored. According to the weight function, the value of $w(0,1)$, $w(1,0)$, $w(1,1)$, and $w(1,-1)$ can best reflect the level of mutual coupling effects. The array inter-element spacing of the first two is equal to unit inter-element spacing, which is the smallest spacing in the array. The other two are spaced by $\sqrt{2}$ times the inter-element spacing. The less the value of $\mathbf{W}$ is, the smaller the mutual coupling effect is, and the DOA estimation performance will be better. Obviously, if we have $\mathbf{W} = (0,0,0,0)$, the array is least affected by mutual coupling.

To reduce mutual coupling, the proposed array can be designed to satisfy the condition of $w(0,1) = 0$ and $w(1,0) = 0$. According to (16), the array elements are defined to have an ascending ordinal number. $w(0,1) = 0$ can be expressed as $\eta_i - \eta_j \neq -1, i < j, i, j \in [1, N]$. Hence, the condition in (16) is strengthened to $\eta_i + 2 \leq \eta_{i+1}, i \in [1, N-1]$. It is not difficult to find that $w(1,0) = 0$ is equivalent to $\eta_i - \eta_j \neq -Q, i < j, i, j = [1, N]$. We can construct a matrix $\mathbf{G}$ as follows

$$\mathbf{G} = \left[\mathbf{G}_1^T, \mathbf{G}_2^T, ..., \mathbf{G}_N^T\right]^T \tag{35}$$

where $\mathbf{G}_n^T = \left[\mathbf{O}_{N-n,2(n-1)}, -\mathbf{v}^{'} \odot \mathbf{1}_{N-n}, \mathbf{I}_{N-n} \otimes \mathbf{v}^{'}\right], n \in [1, N-1]$ with $\mathbf{v}^{'} = [Q, 1]$. The disjunctive optimization problem in (25) can be extended as

$$\begin{aligned} \min \quad & x_N \\ \text{s.t.} \quad & \mathbf{BL} \geq 2 \times \mathbf{1}_{N-1} \\ & \Omega\left(\hat{\mathbf{u}}^{(d)}\mathbf{L} \neq \check{\mathbf{u}}^{(d)}\mathbf{L}\right) = True \quad d = 1, ..., D \\ & \Omega\left(\hat{\mathbf{g}}^{(h)}\mathbf{L} \neq Q\right) = True \quad h = 1, ..., H \end{aligned} \tag{36}$$

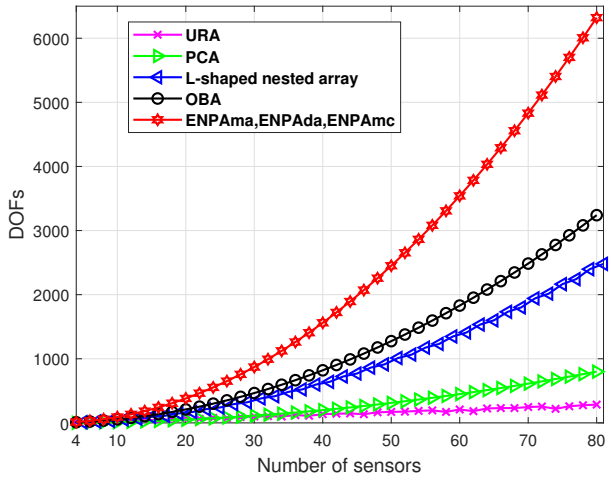

Fig. 4. Achievable DOFs of different arrays.

where $\hat{\mathbf{g}}^{(h)}$ represents the hth row of $\mathbf{G}$. Furthermore, the disjunctive optimization problem in (27) can be reformulated as given in (37).

Considering that the convex hull and the big M-representation own the same solution, we use the latter with fewer variables to solve the MILP optimization problem, which is expressed as

$$\begin{aligned} \min_{\forall \delta_d,\varepsilon_h \in \{0,1\}, d\in[1,D], h\in[1,H]} \quad & x_N \\ \text{s.t.} \quad & Q = \bar{Q} \\ & \mathbf{BL} \geq 2 \times \mathbf{1}_{N-1} \\ & \mathbf{f}^{(d)}\mathbf{L} \geq 1 - M\delta_d \\ & -1 + M(1-\delta_d) \geq \mathbf{f}^{(d)}\mathbf{L} \\ & \hat{\mathbf{g}}^{(h)}\mathbf{L} \geq Q + 1 - M\varepsilon_h \\ & Q - 1 + M(1-\varepsilon_h) \geq \hat{\mathbf{g}}^{(h)}\mathbf{L} \end{aligned} \tag{38}$$

Obviously, the designed array in (38) not only enjoys the property of zero redundancy, but also reduces the mutual coupling effect significantly with $w(0,1)=0$ and $w(1,0)=0$.

Similarly, if the mutual coupling effect needs to be further reduced, we can add more constraints like $w(1,1)=0$ and $w(1,-1)=0$ in weight functions, which is equivalent to $\eta_i - \eta_j \neq -Q \pm 1, i<j, i,j \in [1,N]$. Thus, the inequalities constraint in (37) can be modified to $\hat{\mathbf{g}}^{(h)}\mathbf{L} \leq Q-2$ and $\hat{\mathbf{g}}^{(h)}\mathbf{L} \geq Q+2$. Under a fixed Q, we can design the array for the minimum area with no redundancy and low mutual coupling effect. The specific problem formulation is given by

$$\begin{aligned} \min_{\forall \delta_d,\varepsilon_h \in \{0,1\}, d\in[1,D], h\in[1,H]} \quad & x_N \\ \text{s.t.} \quad & Q = \bar{Q} \\ & \mathbf{BL} \geq 2 \times \mathbf{1}_{N-1} \\ & \mathbf{f}^{(d)}\mathbf{L} \geq 1 - M\delta_d \\ & -1 + M(1-\delta_d) \geq \mathbf{f}^{(d)}\mathbf{L} \\ & \hat{\mathbf{g}}^{(h)}\mathbf{L} \geq Q + 2 - M\varepsilon_h \\ & Q - 2 + M(1-\varepsilon_h) \geq \hat{\mathbf{g}}^{(h)}\mathbf{L} \end{aligned} \tag{39}$$

V. Simulation Results

Numerical examples are provided to demonstrate the performance of the proposed designs. The existing URA, PCA, cross-shaped array, L-shaped nested array, and open box array (OBA) are employed for comparison. The number of antennas of each array configuration in the simulation is kept the same. The signal-to-noise ratio (SNR) is defined as $\mathrm{SNR} = 10\log_{10}(\sigma_s^2/\sigma_n^2)$, where σ_s^2 stands for the power of each source and σ_n^2 represents the power of noise. In particular, the root-mean-square error (RMSE) is used to measure the performance of the designed arrays, which is expressed as

$$\mathrm{RMSE} = \sqrt{\frac{1}{MK}\sum_{m=1}^{M}\sum_{k=1}^{K}\left((\hat{\theta}_m(k)-\theta_m)^2 + (\hat{\varphi}_m(k)-\varphi_m)^2\right)} \tag{40}$$

where M stands for the number of Monte Carlo experiments, and $\left(\hat{\theta}_m(k), \hat{\varphi}_m(k)\right)$ denotes the mth estimate of (θ_m, φ_m) for the kth source.

A. Simulation 1

In the first simulation, we focus on DOFs and mutual coupling, which are important for the array configuration [46]. The curves for the number of DOFs for URA, PCA, L-shaped nested array, OBA, and the proposed arrays are shown in Fig. 4. The closed-form expressions for these existing arrays can be found in [51]. Obviously, the three kinds of proposed non-redundant planar arrays have a larger number of DOFs than the others. Without any redundancy, the proposed array configurations reach the highest number of DOFs, which is $N^2-(N-1)$.

Both weight functions and mutual coupling matrices are considered to show the mutual coupling effects of the proposed arrays, and several typical arrays are analyzed, including URA, PCA, L-shaped nested array, cross-shaped array, OBA, the enhanced non-redundant planar array with minimum area ($\mathrm{ENPA_{ma}}$), the enhanced non-redundant planar array with determined area ($\mathrm{ENPA_{da}}$), and the enhanced non-redundant planar array with reduced mutual coupling ($\mathrm{ENPA_{mc}}$). The number of array elements is fixed at 9 for all. The three proposed array structures are shown in Fig. 5. The black circles denote the physical antennas and the red crosses stand for holes. The value of Q is fixed at 6. The pre-determined array area is $\bar{P}=7$ in Fig. 5 (b). The mutual coupling constraint is satisfied with $\mathbf{W}=(0,0,0,0)$ in Fig. 5 (c).

In Fig. 6, we use red circles to mark the values in $\mathbf{W}$, because these cases characterize the severity of mutual coupling effects. Based on the dense inter-element spacing, the value of weight functions is large in URA. Compared to the URA, the OBA owns smaller weight functions ($\mathbf{W}=(4,4,2,2)$). The L-shaped nested array ($\mathbf{W}=(2,2,1,1)$), the cross-shaped array ($\mathbf{W}=(2,2,0,0)$), and the PCA can also achieve smaller weight functions with larger inter-element spacing. Due to the non-redundancy property, the value of the weight functions is equal to 1 at most except for $w(0,0)$, and the mutual coupling effect is further reduced in the proposed $\mathrm{ENPA_{ma}}$ ($\mathbf{W}=(1,1,1,1)$) and the proposed $\mathrm{ENPA_{da}}$

$$\begin{aligned} \min_{\forall \delta_d,\varepsilon_h \in \{0,1\}, d\in[1,D], h\in[1,H]} \quad & x_N \\ \text{s.t.} \quad & \mathbf{BL} \geq 2 \times \mathbf{1}_{N-1} \\ & \begin{bmatrix} \delta_d \\ \mathbf{f}^{(d)}\mathbf{L} \leq -1 \end{bmatrix} \vee \begin{bmatrix} 1-\delta_d \\ \mathbf{f}^{(d)}\mathbf{L} \geq 1 \end{bmatrix} \\ & \begin{bmatrix} \varepsilon_h \\ \hat{\mathbf{g}}^{(h)}\mathbf{L} \leq Q-1 \end{bmatrix} \vee \begin{bmatrix} 1-\varepsilon_h \\ \hat{\mathbf{g}}^{(h)}\mathbf{L} \geq Q+1 \end{bmatrix} \end{aligned} \tag{37}$$

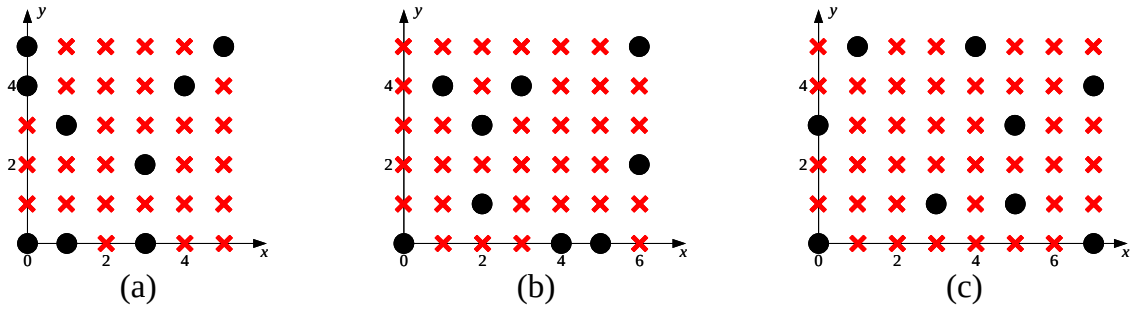

Fig. 5. The proposed array structures with 9 elements: (a) $\mathrm{ENPA_{ma}}$, (b) $\mathrm{ENPA_{da}}$, and (c) $\mathrm{ENPA_{mc}}$.

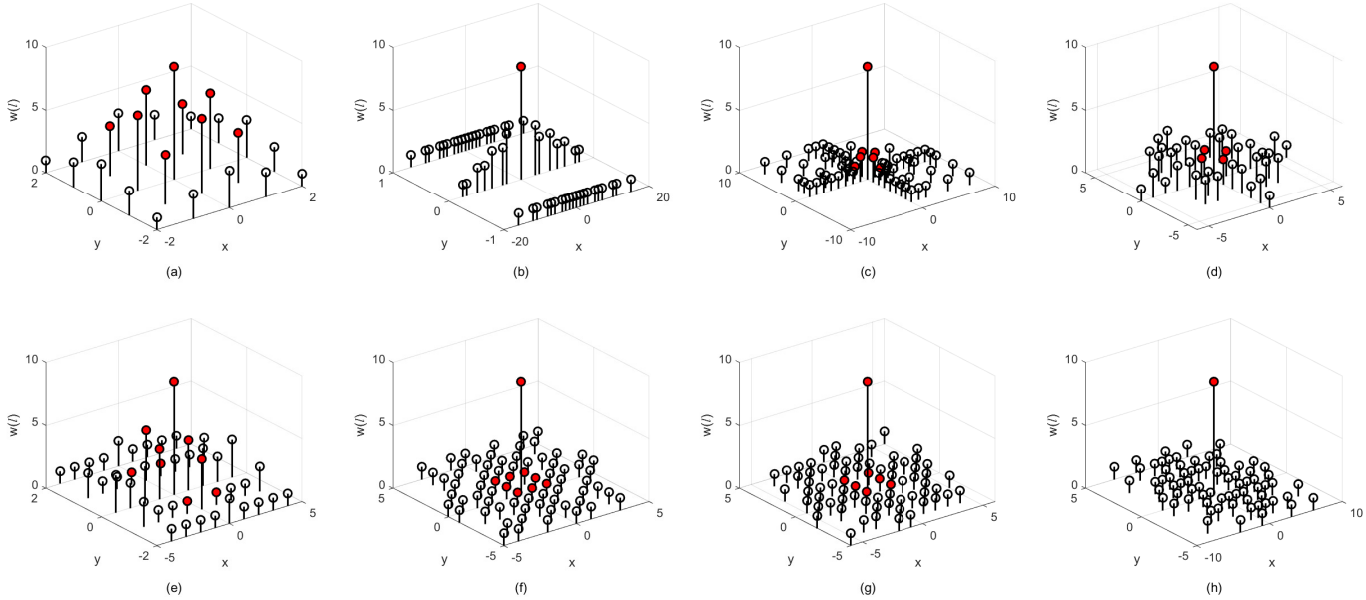

Fig. 6. Weight functions for eight different 9-element arrays: (a) URA, (b) PCA, (c) L-shaped nested array, (d) Cross-shaped array, (e) OBA, (f) $\mathrm{ENPA_{ma}}$, (g) $\mathrm{ENPA_{da}}$, and (h) $\mathrm{ENPA_{mc}}$ (The red circles mark the values in $\mathbf{W}$).

$(\mathbf{W} = (0, 1, 1, 1))$. Considering that the purpose of designing $\mathrm{ENPA_{mc}}$ $(\mathbf{W} = (0, 0, 0, 0))$ is to suppress the mutual coupling effects, it has the best performance in Fig. 6.

Fig. 7 shows the magnitudes of the mutual coupling matrices. We consider eight different array configurations with 9 elements. It is a visual representation of the matrix $\mathbf{C}$. The deeper the blue color is, the smaller the mutual coupling. Different arrays have the same value $(c_0 = 1)$ in the diagonal elements, and the magnitudes are also the highest. The property of URA is the worst due to small inter-element spacing. Obviously, the proposed $\mathrm{ENPA_{mc}}$ achieves the best performance with smallest magnitudes.

B. Simulation 2

In this subsection, the performance of DOA estimation in the absence of mutual coupling is examined versus SNR and the number of snapshots. We utilize sparse reconstruction algorithms, and the number of array elements is still fixed at 9. Assume that there are two sources located at $(45°, 32°)$ and $(55°, 38°)$. The eight array structures are kept the same as in Simulation 1. The number of Monte-Carlo trials is 800.

Fig. 8 shows RMSE performance versus SNR in the absence of mutual coupling. The regularization parameter $\mu = 2.5$ for the sparse reconstruction algorithm. The number of snapshots is 500, and the grid step size is $0.1°$. The curves of the three

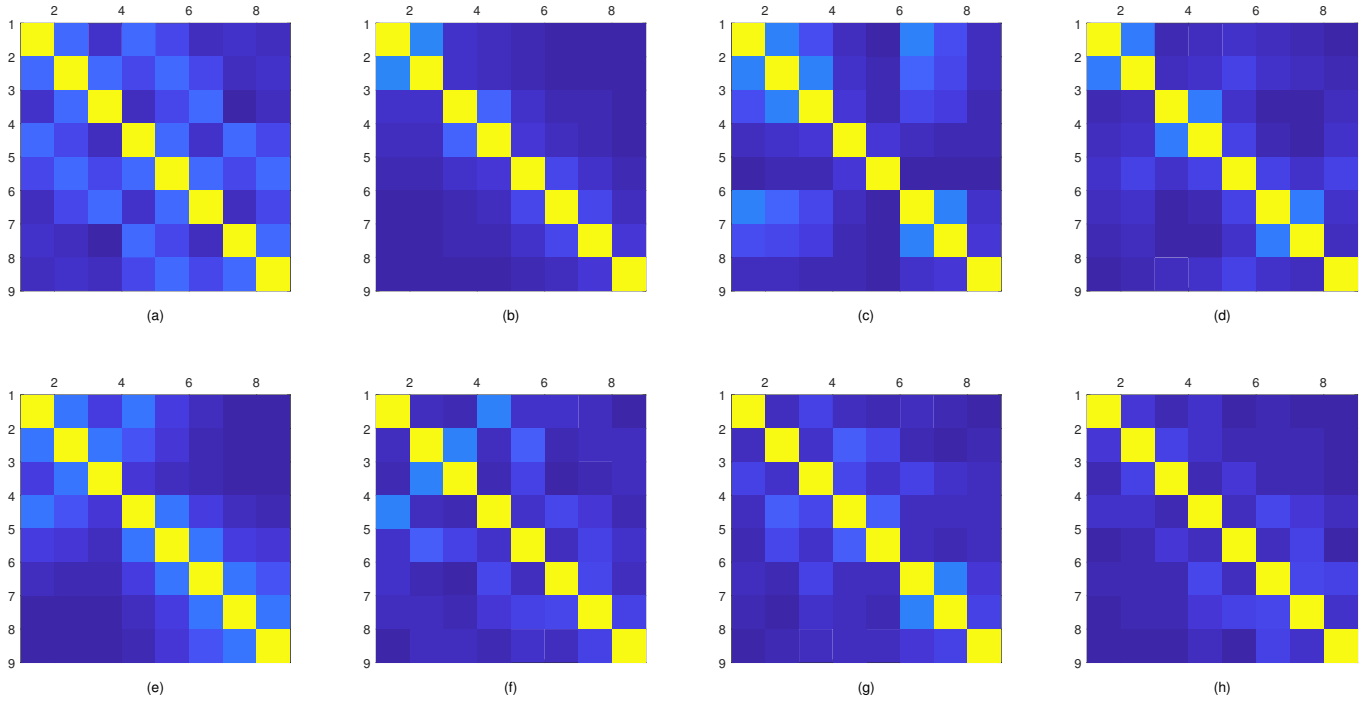

Fig. 7. Magnitudes of the mutual coupling matrices for different kinds of 9-element arrays: (a) URA, (b) PCA, (c) L-shaped nested array, (d) Cross-shaped array, (e) OBA, (f) $\mathrm{ENPA_{ma}}$, (g) $\mathrm{ENPA_{da}}$, and (h) $\mathrm{ENPA_{mc}}$.

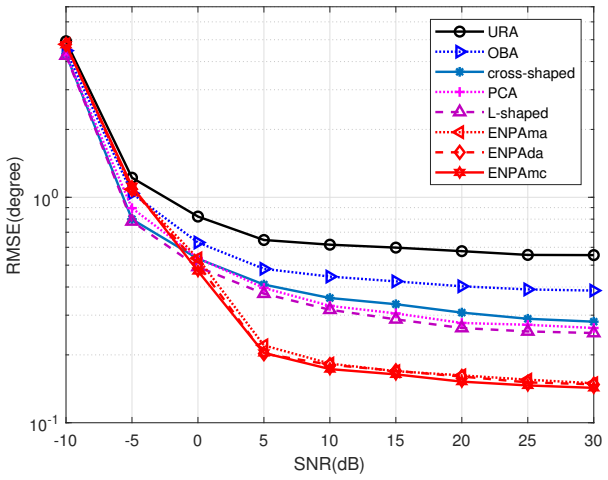

Fig. 8. RMSE of DOA versus SNR in the absence of mutual coupling.

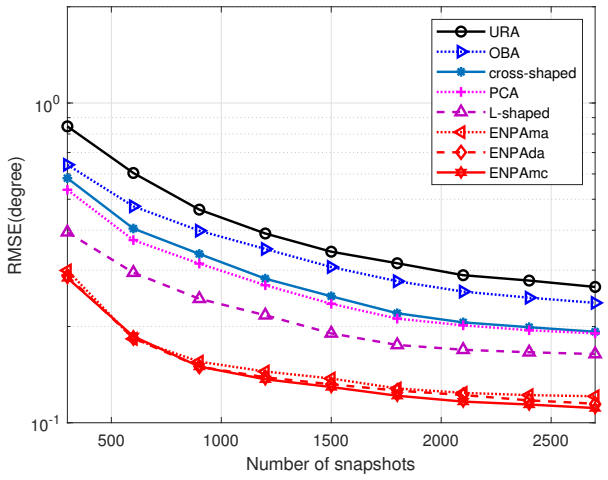

Fig. 9. RMSE of DOA versus the number of snapshots in the absence of mutual coupling.

proposed enhanced non-redundant planar arrays is quite close to each other. They can achieve better RMSE than the other array configurations when $\mathrm{SNR} > 0\mathrm{dB}$. However, at low SNRs, as expected, the performance of the designed arrays is poor.

In Fig. 9, we show the performance of DOA estimation versus snapshots without mutual coupling effects. SNR is $10\mathrm{dB}$ and, the range of snapshots is from 300 to 2700, with intervals of 300. Obviously, the higher the number of snapshots, the better the performance. Moreover, the three types of proposed arrays provide better estimation performance than other existing arrays.

C. Simulation 3

In this simulation, the DOA estimation performance in the presence of mutual coupling is demonstrated. The mutual coupling parameters are set as $c(1) = 0.3$, $c(l) = c(1)e^{j\pi(l-1)/4}/l$, and $B = 10$. The RMSE performance versus SNR is presented in Fig. 10. Fig. 11 shows the performance versus snapshots.

In Fig. 10, the URA cannot work properly due to the large mutual coupling effects between different antennas. The proposd $\mathrm{ENPA_{mc}}$ has smaller RMSE than other configurations because of the reduced mutual coupling design. Similarly, the

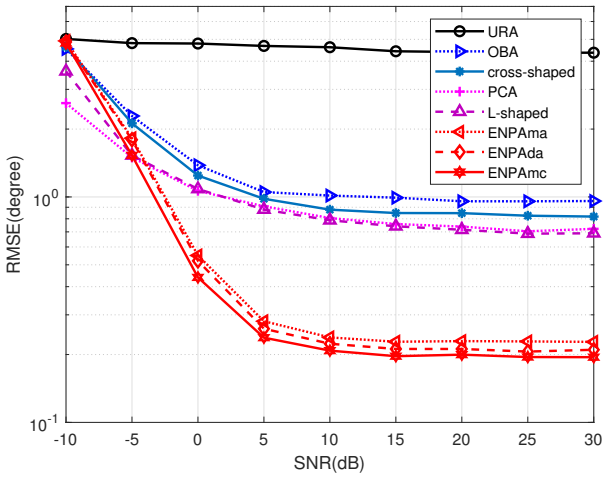

Fig. 10. RMSE of DOA versus SNR in the presence of mutual coupling.

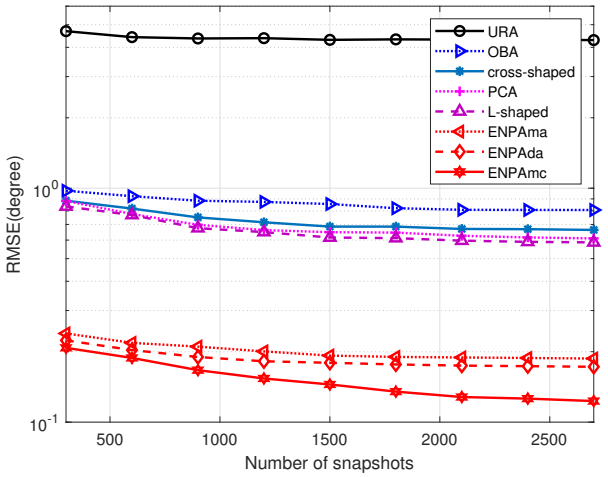

Fig. 11. RMSE of DOA versus the number of snapshots in the presence of mutual coupling.

performance of the three non-redundant arrays is better than other array configurations for different snapshots according to Fig. 11.

VI. Conclusions

In this paper, a framework for non-redundant sparse planar array design has been proposed. The designed arrays can achieve the maximum possible DOFs due to no redundancies in the generated virtual arrays. The rule for non-redundant design of planar arrays was first introduced, which is also the basic design criterion. According to GDP, the enhanced non-redundant sparse planar array design was developed. Furthermore, two types of MILP optimization approaches, the convex hull and the big M-representation, were considered. Then, taking different application conditions into consideration, three kinds of non-redundant sparse planar arrays were designed for minimum array area, pre-determined array area, and reduced mutual coupling, respectively. Simulation results have demonstrated the superior performance of the proposed planar array configurations for DOA estimation, especially in the presence of mutual coupling effects.

References

[1] H. Krim and M. Viberg, "Two decades of array signal processing research: the parametric approach," *IEEE Signal Process. Mag.*, vol. 13, no. 4, pp. 67–94, 1996.

[2] H. L. V. Trees, *Optimum Array Processing: Part IV of Detection,Estimation, and Modulation Theory*. Wiley Interscience, 2002.

[3] F.-J. Chen, S. Kwong, and C.-W. Kok, "ESPRIT-like two-dimensional DOA estimation for coherent signals," *IEEE Trans. Aerosp. Electron. Syst.*, vol. 46, no. 3, pp. 1477–1484, 2010.

[4] J. Shi, G. Hu, X. Zhang, F. Sun, and H. Zhou, "Sparsity-based two-dimensional DOA estimation for coprime array: From sum-difference coarray viewpoint," *IEEE Trans. Signal Process.*, vol. 65, no. 21, pp. 5591–5604, 2017.

[5] Q. Wu, F. Sun, P. Lan, G. Ding, and X. Zhang, "Two-dimensional direction-of-arrival estimation for co-prime planar arrays: A partial spectral search approach," *IEEE Sensors J.*, vol. 16, no. 14, pp. 5660–5670, 2016.

[6] F. Wen, G. Gui, H. Gacanin, and H. Sari, "Compressive sampling framework for 2d-doa and polarization estimation in mmwave polarized massive mimo systems," *IEEE Trans. Wireless Commun.*, vol. 22, no. 5, pp. 3071–3083, 2023.

[7] F. Wen, J. Shi, G. Gui, H. Gacanin, and O. A. Dobre, "3-d positioning method for anonymous uav based on bistatic polarized mimo radar," *IEEE Int. Things J.*, vol. 10, no. 1, pp. 815–827, 2023.

[8] Z. Zhang, F. Wen, J. Shi, J. He, and T.-K. Truong, "2D-DOA estimation for coherent signals via a polarized uniform rectangular array," *IEEE Signal Process. Lett.*, vol. 30, pp. 893–897, 2023.

[9] Y. Zhang and L. Jiang, "A direct data approach to joint 2D-DOA and frequency estimation with L-shaped array," *IEEE Trans. Aerosp. Electron. Syst.*, pp. 1–11, 2022.

[10] B. Friedlander and A. Weiss, "Direction finding in the presence of mutual coupling," *IEEE Trans. Antennas Propagat.*, vol. 39, no. 3, pp. 273–284, 1991.

[11] W. Zheng, X. Zhang, Y. Wang, M. Zhou, and Q. Wu, "Extended coprime array configuration generating large-scale antenna co-array in massive MIMO system," *IEEE Trans. Veh. Technol.*, vol. 68, no. 8, pp. 7841–7853, 2019.

[12] J. He, L. Li, and T. Shu, "Sparse nested arrays with spatially spread square acoustic vector sensors for high-accuracy underdetermined direction finding," *IEEE Trans. Aerosp. Electron. Syst.*, vol. 57, no. 4, pp. 2324–2336, 2021.

[13] J. Shi, F. Wen, Y. Liu, Z. Liu, and P. Hu, "Enhanced and generalized coprime array for direction of arrival estimation," *IEEE Trans. Aerosp. Electron. Syst.*, vol. 59, no. 2, pp. 1327–1339, 2023.

[14] H. Zheng, C. Zhou, Z. Shi, Y. Gu, and Y. D. Zhang, "Coarray tensor direction-of-arrival estimation," *IEEE Trans. Signal Process.*, vol. 71, pp. 1128–1142, 2023.

[15] C. Zhou, Y. Gu, Z. Shi, and M. Haardt, "Structured nyquist correlation reconstruction for DOA estimation with sparse arrays," *IEEE Trans. Signal Process.*, vol. 71, pp. 1849–1862, 2023.

[16] J. Shi, G. Hu, X. Zhang, and F. Sun, "Sparsity-based DOA estimation of coherent and uncorrelated targets with flexible MIMO radar," *IEEE Trans. Veh. Technol.*, vol. 68, no. 6, pp. 5835–5848, 2019.

[17] P. P. Vaidyanathan and P. Pal, "Sparse sensing with co-prime samplers and arrays," *IEEE Trans. Signal Process.*, vol. 59, no. 2, pp. 573–586, 2011.

[18] P. Pal and P. P. Vaidyanathan, "Nested arrays: A novel approach to array processing with enhanced degrees of freedom," *IEEE Trans. Signal Process.*, vol. 58, no. 8, pp. 4167–4181, 2010.

[19] Z. Zheng, W.-Q. Wang, Y. Kong, and Y. D. Zhang, "MISC array: A new sparse array design achieving increased degrees of freedom and reduced mutual coupling effect," *IEEE Trans. Signal Process.*, vol. 67, no. 7, pp. 1728–1741, 2019.

[20] W. Zheng, X. Zhang, Y. Wang, J. Shen, and B. Champagne, "Padded coprime arrays for improved DOA estimation: Exploiting hole representation and filling strategies," *IEEE Trans. Signal Process.*, vol. 68, pp. 4597–4611, 2020.

[21] W. Zheng, X. Zhang, J. Li, and J. Shi, "Extensions of co-prime array for improved DOA estimation with hole filling strategy," *IEEE Sensors J.*, vol. 21, no. 5, pp. 6724–6732, 2021.

[22] P. Gupta and M. Agrawal, "Design and analysis of the sparse array for DoA estimation of noncircular signals," *IEEE Trans. Signal Process.*, vol. 67, no. 2, pp. 460–473, 2019.
[23] S. Qin, Y. D. Zhang, and M. G. Amin, "Two-dimensional DOA estimation using parallel coprime subarrays," in *2016 IEEE Sensor Array and Multichannel Signal Processing Workshop (SAM)*, 2016, pp. 1–4.
[24] J. He, L. Li, and T. Shu, "2-D direction finding using parallel nested arrays with full co-array aperture extension," *Signal Process.*, vol. 178, p. 107795, 2021.
[25] Z. Zheng, Y. Yang, W.-Q. Wang, and S. Zhang, "Two-dimensional direction estimation of multiple signals using two parallel sparse linear arrays," *Signal Process.*, vol. 143, pp. 112–121, 2018.
[26] S. Qin, Y. D. Zhang, and M. G. Amin, "Improved two-dimensional DOA estimation using parallel coprime arrays," *Signal Process.*, vol. 172, p. 107428, 2020.
[27] L. Liang, Y. Shi, Y. Shi, Z. Bai, and W. He, "Two-dimensional DOA estimation method of acoustic vector sensor array based on sparse recovery," *Digit. Signal Process.*, vol. 120, p. 103294, 2022.
[28] P. Ma, J. Li, G. Zhao, and X. Zhang, "Computation-efficient 2-D DOA estimation algorithm with array motion strategy," *Digit. Signal Process.*, vol. 112, p. 103013, 2021.
[29] J. Li, J. Zhao, Y. Ding, Y. Li, and F. Chen, "An improved co-prime parallel array with conjugate augmentation for 2-D DOA estimation," *IEEE Sens. J.*, vol. 21, no. 20, pp. 23 400–23 411, 2021.
[30] X. Wu and W.-P. Zhu, "Single far-field or near-field source localization with sparse or uniform cross array," *IEEE Trans. Veh. Technol.*, vol. 69, no. 8, pp. 9135–9139, 2020.
[31] Y. Hua, T. Sarkar, and D. Weiner, "An L-shaped array for estimating 2-D directions of wave arrival," *IEEE Trans. Antennas Propagat.*, vol. 39, no. 2, pp. 143–146, 1991.
[32] C. Jian, S. Wang, and L. Lin, "2-D DOA estimation by minimum-redundancy linear array," *8th International Conference on Signal Processing, Guilin*, pp. 393+, 2006.
[33] Y.-Y. Dong, C.-X. Dong, Y.-T. Zhu, G.-Q. Zhao, and S.-Y. Liu, "Two-dimensional DOA estimation for L-shaped array with nested subarrays without pair matching," *IET Signal Process.*, vol. 10, no. 9, pp. 1112–1117, Dec 2016.
[34] X. Wu and W.-P. Zhu, "V-shaped sparse arrays for 2-D DOA estimation," *Circuits, Syst., Signal Process.*, vol. 38, no. 6, pp. 2792–2809, Jun 2019.
[35] R. A. Haubrich, "Array design," *Seismol. Soc. Am., Bull.*, vol. 58, no. 3, pp. 977–991, 1968.
[36] C.-L. Liu and P. P. Vaidyanathan, "Hourglass arrays and other novel 2-D sparse arrays with reduced mutual coupling," *IEEE Trans. Signal Process.*, vol. 65, no. 13, pp. 3369–3383, 2017.
[37] A. Moffet, "Minimum-redundancy linear arrays," *IEEE Trans. Antennas Propagat.*, vol. 16, no. 2, pp. 172–175, 1968.
[38] A. Ahmed and Y. D. Zhang, "Generalized non-redundant sparse array designs," *IEEE Trans. Signal Process.*, vol. 69, pp. 4580–4594, 2021.
[39] E. Vertatschitsch and S. Haykin, "Nonredundant arrays," *Proc. IEEE*, vol. 74, no. 1, pp. 217–217, 1986.
[40] D. Linebarger, I. Sudborough, and I. Tollis, "Difference bases and sparse sensor arrays," *IEEE Trans. Inf. Theory*, vol. 39, no. 2, pp. 716–721, 1993.
[41] J. Arsac and A. Danjon, "Nouveau reseau pour lobservation radioastronomique de la brillance sur le soleil a 9350 Mc/s," *C.R.Acad.Sci.*, vol. 240, no. 9, pp. 942–945, 1955.
[42] I. E. Grossmann and J. P. Ruiz, "Generalized disjunctive programming: A framework for formulation and alternative algorithms for MINLP optimization," *Mixed Integer Nonlinear Programming*, vol. 154, pp. 93–115, 2012.
[43] E. Balas, *Disjunctive Programming*. Springer, 2018.
[44] J. Kallrath, "Mixed integer optimization in the chemical process industry: Experience, potential and future perspectives," *Trans. I .Chem E.*, vol. 78, no. 6, pp. 809–822, 2000.
[45] C. A. Mendez, J. Cerda, I. E. Grossmann, I. Harjunkoski, and M. Fahl, "State-of-the-art review of optimization methods for short-term scheduling of batch processes," *Comput. Chem. Eng.*, vol. 30, no. 6-7, pp. 913–946, May 15 2006.
[46] C.-L. Liu and P. P. Vaidyanathan, "Super nested arrays: Linear sparse arrays with reduced mutual coupling–part I: Fundamentals," *IEEE Trans. Signal Process.*, vol. 64, no. 15, pp. 3997–4012, 2016.
[47] D. Malioutov, M. Cetin, and A. Willsky, "A sparse signal reconstruction perspective for source localization with sensor arrays," *IEEE Trans. Signal Process.*, vol. 53, no. 8, pp. 3010–3022, 2005.
[48] Q. Shen, W. Liu, W. Cui, and S. Wu, "Underdetermined DOA estimation under the compressive sensing framework: A review," *IEEE Access*, vol. 4, pp. 8865–8878, 2016.
[49] Gurobi, "Gurobi optimizer reference manual." [Online]. Available: http://www.gurobi.com
[50] MosekApS, "The MOSEK optimization toolbox for MATLAB manual. version 9.0." 2019. [Online]. Available: http://docs.mosek.com/9.0/toolbox/index.html
[51] I. Aboumahmoud, A. Muqaibel, M. Alhassoun, and S. Alawsh, "A review of sparse sensor arrays for two-dimensional direction-of-arrival estimation," *IEEE Access*, vol. 9, pp. 92 999–93 017, 2021.

Hangqi Yan (Student Member, IEEE) received the B.Sc. degree in electronics and information engineering in 2019 from Northwestern Polytechnical University, Xi'an, China, where he is currently working toward the Ph.D. degree in information and communication engineering. His current research interests include array signal processing, parameter estimation, and their applications.

Yuexian Wang (Member, IEEE) received the B.Sc. degree in electronics and information engineering from Northwestern Polytechnical University, China, in 2006, and the M.Eng. and Ph.D. degrees in electrical and electronic engineering from The University of Adelaide, Australia, in 2012 and 2015, respectively, where he was a Postdoctoral Fellow, from 2015 to 2017. Since 2018, he has been with the School of Electronics and Information, Northwestern Polytechnical University, where he is currently an Associate Professor. His research interests include array signal processing, compressed sensing, and their applications to radar, sonar, and wireless communications.

Ling Wang (Member, IEEE) received the B.Sc., M.Sc., and Ph.D. degrees in electronic engineering from Xidian University, Xi'an, China, in 1999, 2002, and 2004, respectively. From 2004 to 2007, he was with Siemens and Nokia Siemens Networks, Espoo, Finland. Since 2007, he has been with Northwestern Polytechnical University as a professor. Currently, he serves as the dean of school of electronics and information and he is a recipient of the national talents award. His current research interests include array processing and smart antennas, wideband communications, cognitive radio, adaptive anti-jamming for satellite communications, satellite navigation, and date link systems.

Rongfeng Li received M.S. in underwater acoustics engineering from the China Ship Research and Development Academy in 2006. He has been successively engaged in system design, ship information, and modern service and management science at Hangzhou Applied Acoustics Research Institute, CSSC. His current main research interest is modern service and management science.

Wei Liu (S'01-M'04-SM'10) received his BSc (Space Physics) and LLB (Intellectual Property Law) degrees from Peking University, China, in 1996 and 1997, respectively, MPhil from the Department of Electrical and Electronic Engineering, University of Hong Kong in 2001, and PhD from the School of Electronics and Computer Science, University of Southampton, UK, in 2003. He then worked as a postdoc first at Southampton and later at Imperial College London. In September 2005, he joined the Department of Electronic and Electrical Engineering, University of Sheffield, UK, first as a Lecturer and then a Senior Lecturer. Since September 2023, he has been a Reader at the School of Electronic Engineering and Computer Science, Queen Mary University of London, UK. He has published 400+ journal and conference papers, five book chapters, and two research monographs titled "Wideband Beamforming: Concepts and Techniques" (Wiley, March 2010) and "Low-Cost Smart Antennas" (Wiley, March 2019), respectively. His research interests cover a wide range of topics in signal processing, with a focus on sensor array signal processing and its various applications, such as robotics and autonomous systems, human computer interface, radar, sonar, and wireless communications.

He is a member of the Digital Signal Processing Technical Committee of the IEEE Circuits and Systems Society (Chair for 2022-2024), the Sensor Array and Multichannel Signal Processing Technical Committee of the IEEE Signal Processing Society (SPS) (Chair for 2021-2022), the IEEE SPS Technical Directions Board (2021-2022), and the IEEE SPS Conference Board (2022-2023). He also acted as an associate editor for IEEE Trans. on Signal Processing, IEEE Access, and Journal of the Franklin Institute, and currently he is an associate editor for IEEE Antennas and Wireless Propagation Letters, and an Executive Associate Editor-in-Chief of the Frontiers of Information Technology and Electronic Engineering. He is an IEEE Distinguished Lecturer for the Aerospace and Electronic Systems Society (2023-2024).